THE JOURNAL OF BIOLOGICAL CHEMISTRY VOL. 285, NO. 22, pp. 16874–16879, May 28, 2010
Printed in the U.S.A.

Interaction between DNA Polymerase λ and Anticancer Nucleoside Analogs*

Received for publication, December 18, 2009, and in revised form, March 12, 2010 Published, JBC Papers in Press, March 26, 2010, DOI 10.1074/jbc.M109.094391

Miguel Garcia-Diaz[‡1], **Michael S. Murray**[‡], **Thomas A. Kunkel**[‡], **and Kai-ming Chou**[§2]

From the [‡]*Laboratory of Structural Biology and Laboratory of Molecular Genetics, NIEHS, National Institutes of Health, Department of Health and Human Services, Research Triangle Park, North Carolina 27709 and the* [§]*Department of Pharmacology and Toxicology, Indiana University School of Medicine, Indianapolis, Indiana 46202*

The anticancer activity of cytarabine (AraC) and gemcitabine (dFdC) is thought to result from chain termination after incorporation into DNA. To investigate their incorporation into DNA at atomic level resolution, we present crystal structures of human DNA polymerase λ (Pol λ) bound to gapped DNA and containing either AraC or dFdC paired opposite template dG. These structures reveal that AraC and dFdC can bind within the nascent base pair binding pocket of Pol λ. Although the conformation of the ribose of AraCTP is similar to that of normal dCTP, the conformation of dFdCTP is significantly different. Consistent with these structures, Pol λ efficiently incorporates AraCTP but not dFdCTP. The data are consistent with the possibility that Pol λ could modulate the cytotoxic effect of AraC.

Nucleoside analogs are an important class of compounds that are clinically used for anticancer and antiviral treatments (1). For example, 3TC,[3] AZT, and D4T have been used for antiviral treatments (1). AraC (Fig. 1) is used to treat leukemia (2), and dFdC (Fig. 1) is used to treat various types of cancer, such as non-small cell lung cancer (3), breast cancer (4), and pancreatic cancer (5). The main mechanism of action of nucleoside analogs is to terminate the DNA elongation process after their incorporation into viral or cellular DNA (6–8). For example, due to the lack of a 3′-hydroxyl group on their sugar moieties, the incorporation of the antiviral compounds 3TC, AZT, and D4T terminates human immunodeficiency virus DNA replication immediately (9). Although both AraC and gemcitabine have a 3′-hydroxyl group on their sugar moieties, the incorporation of either compound has been shown to terminate the DNA elongation processes and result in DNA fragmentation (7, 10). Studies have shown that the arabinose sugar moiety in AraC and the difluoro group on the 2′-position of the sugar moiety of dFdC alter the DNA structure, inhibiting DNA polymerases (11, 12). The cytotoxicity of AraC or dFdC is proportional to the amount of the analog incorporated into DNA (6–8). Therefore, the cellular enzymes that are involved in activating these nucleoside analogs and the DNA polymerases that introduce them into DNA play a critical role in determining their cytotoxic activity.

Human DNA polymerase λ (Pol λ) is an exonuclease-deficient, 575-amino acid DNA polymerase that belongs to the X-family (13). It contains a N-terminal BRCT domain that is important for protein partnerships, a proline/serine-rich region that has been suggested to be a target for post-translational modification, and a C-terminal 39-kDa polymerase domain (14). The 39-kDa domain, which is structurally well characterized (15, 16) contains the fingers, palm, and thumb subdomains typical of DNA polymerases (17). It also contains an 8-kDa subdomain with dRP lyase activity (14) that contributes to base excision repair (BER) *in vitro*. Studies in Pol β-deficient mouse embryonic fibroblast extracts indicate that Pol λ also performs BER *in vivo* (18, 19). Moreover, in a confocal microscopy study, Pol λ relocates to sites of oxidative DNA damage, and embryonic fibroblasts derived from the Pol λ knock-out mice are more sensitive than wild type cells to H_2O_2 treatments (18). These studies suggested that Pol λ plays a protective role against oxidative DNA damage. A recent report further indicates that expression of Pol λ increases in order to repair smoking-induced damage in respiratory epithelium (20). In addition to BER, Pol λ is also strongly implicated in filling gaps in DNA during non-homologous end joining of double strand breaks (15, 16, 21).

It is therefore possible that Pol λ could incorporate therapeutic nucleoside analogs into DNA during BER and non-homologous end joining, which may have an impact on the cellular sensitivity to these compounds following DNA damage. Therefore, in this study, we investigate the ability of Pol λ to incorporate AraCTP and dFdCTP, and we provide crystal structures of Pol λ in a complex with a physiologically relevant, one-nucleotide gapped DNA substrate with each analog present.

* This work was supported, in whole or in part, by National Institutes of Health (NIH) Grant RO1 CA112446 (to K.-m. C.) and by NIH, NIEHS, Division of Intramural Research Project Z01 ES065070 (to T. A. K.).

The atomic coordinates and structure factors (codes 3MDA and 3MDC) have been deposited in the Protein Data Bank, Research Collaboratory for Structural Bioinformatics, Rutgers University, New Brunswick, NJ (http://www.rcsb.org/).

[1] Present address: Dept. of Pharmacological Sciences, BST 7-169, SUNY at Stony Brook, Stony Brook, NY 11794-8651.

[2] To whom correspondence should be addressed: Dept. of Pharmacology and Toxicology, Indiana University School of Medicine, 635 Barnhill Dr., MS 552, Indianapolis, IN 46202. Tel.: 317-278-8509; E-mail: chouk@iupui.edu.

[3] The abbreviations used are: 3TC, 2′,3′-dideoxy-3′-thiacytidine (lamivudine); AZT, 3′-azido-3′-deoxythymidine (zidovudine); D4T, 2′,3′-didehydro-3′-deoxythymidine (stavudine); AraC, cytosine-1-β-D-arabinofuranoside (cytarabine); dFdC, β-D-2′,2′-difluorodeoxycytidine (gemcitabine); AraCTP, 5′-triphosphate metabolite of AraC; AraCMP, 5′-monophosphate metabolite of AraC; dFdCTP, 5′-triphosphate metabolite of dFdC; dFdCMP, 5′-monophosphate metabolite of AraC; Pol λ, DNA polymerase λ; BER, base excision repair; MEF, mouse embryo fibroblast; PDB, Protein Data Bank.

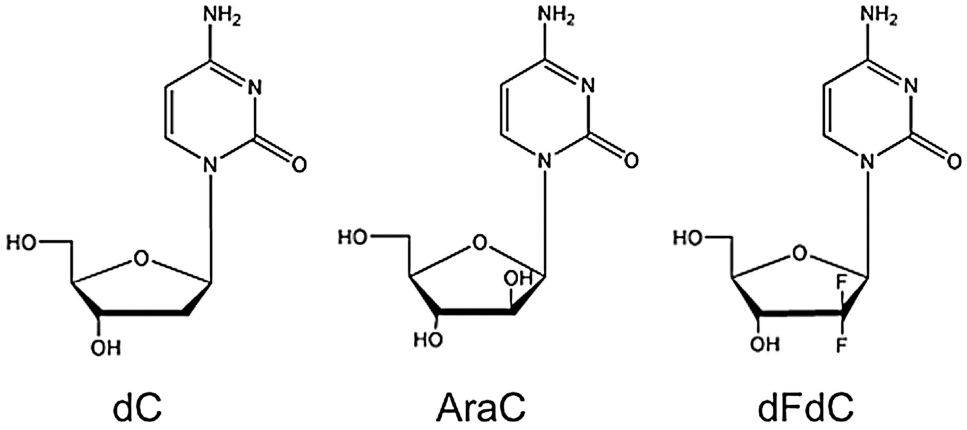

FIGURE 1. **The structures of nucleoside analogs.**

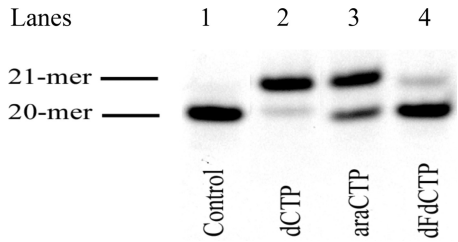

FIGURE 2. **Incorporation of the AraCTP and dFdCTP by Pol λ.** Pol λ was incubated with a double-stranded DNA oligonucleotide containing a single nucleotide gap under the conditions described under "Materials and Methods" in the presence of different nucleoside triphosphates at 37 °C for 5 min. The reactions were analyzed using a denaturing sequencing gel, and the results were visualized with a phosphor imager. The reactions were control DNA without dNTPs (*lane 1*) and in the presence of dCTP (*lane 2*), AraCTP (*lane 3*), and dFdCTP (*lane 4*).

TABLE 1
The kinetic parameters of wild type Pol λ on dCTP and AraCTP

Substrate	k_{cat}	K_m	k_{cat}/K_m
	min^{-1}	μM	
dCTP	6.7 ± 0.5	0.04 ± 0.02	175
AraCTP	5.8 ± 0.7	0.6 ± 0.3	9.7
dFdCTP	2.9 ± 0.4	2.5 ± 1.1	1.2

TABLE 2
Summary of crystallographic data

Parameters	Values	
	PDB entry 3MDA	PDB entry 3MDC
Data collection		
Unit cell dimensions (Å)	56.068 × 62.637 × 140.163	55.206 × 59.773 × 142.008
Space group	$P2_12_12_1$	$P2_12_12_1$
No. of observations	121,905	145,793
Unique reflections	52,786	30,728
R_{sym} (%) (last shell)	5.6 (42.1)	11.4 (54.0)
$I/\sigma I$ (last shell)	19.9 (2.2)	10.1 (2.1)
Completeness (%) (last shell)	91.5 (77.6)	94.4 (86.0)
Refinement statistics		
Resolution (Å)	2.03	2.00
R_{cryst} (%)	19.9 (2.2)	21.62
R_{free} (%)	25.94	26.63
Complexes in asymmetric unit	1	1
Root mean square deviation from ideal values		
Bond length (Å)	0.004	0.006
Bond angle (degrees)	1.255	1.080
Ramachandran statistics		
Residues in favored regions	96.90	96.10
Residues in allowed regions	100	100

MATERIALS AND METHODS

Purification of Pol λ Proteins and Primer Extension Assays—The expression and purification processes of Pol λ protein were as previously described (14). The Pol λ Y505A mutant protein expression vector was generated using the QuikChange site-directed mutagenesis kit (Stratagene) with a forward primer, 5′-TGCCTGTGCCCTGCTCGCTTTCACCGGCTCTGCAC-3′, and a reverse primer, 5′-GTGCAGAGCCGGTGAAAGCGAGCAGGGCACAGGCA-3′, on a pET-22b vector (Merck) that harbors 39-kDa fragment of wild type Pol λ. The sequence was confirmed by sequencing. The Y505A mutant protein was expressed and purified using the same procedures as for the wild type Pol λ (14). To evaluate the polymerase activity of Pol λ, 1.25 nM Pol λ was incubated with 100 nM double-stranded DNA oligonucleotide containing a single nucleotide gap in the presence of 50 μM dNTP, 50 mM Tris-HCl, pH 7.5, 10 mM $MgCl_2$, 1 mM dithiothreitol, 4% glycerol, 0.1 mg/ml bovine serum albumin. For steady state kinetic analysis, the concentrations of the nucleoside triphosphate metabolites were ranged from 0.01 to 50 μM at a fixed enzyme concentration. For each reaction, less than 25% of the substrates were converted to products by the enzyme, even at the lowest substrate concentration. All of the kinetic data were determined based on the initial reaction rates. The reaction mixtures were analyzed with a 12% denaturing polyacrylamide DNA sequencing gel, and the results were quantified with a phosphor imager (Fuji FLA5100).

Cell Lines and Cell Sensitivity Assay—The SV40-transformed Pol $\lambda^{+/+}$ and Pol $\lambda^{-/-}$ MEF cells were a generous gift from Dr. Samuel Wilson (NIEHS, National Institutes of Health) (19). The cells were grown at 37 °C in a 10% CO_2 incubator in Dulbecco's modified Eagle's medium and 10% fetal bovine serum. For cell sensitivity studies, 4,000 cells/well were seeded in a 24-well plate 24 h before adding different concentrations of AraC. The cells were incubated for an additional 72 h in the humidified incubator. At the end of incubation period, 5 mg/ml 3-(4,5-dimethylthiazol-2-yl)-2,5-diphenyltetrazolium bromide (100 μl) was added for an additional 4-h incubation, and the 3-(4,5-dimethylthiazol-2-yl)-2,5-diphenyltetrazolium bromide/formazan generated by live cells was dissolved in 200 μl of DMSO. The absorbance was determined at 560 nm using a microtiter plate reader (Bio-Rad Benchmark Plus). The cell survival data were presented as percentage of the absorbance of treated/untreated cells.

Crystallization—Crystals of Pol λ in complex with oligonucleotides T11 (5′-CGGCGGTACTG), PG (5′-CAGTAC), and DT (5′-GCCG) were grown using the hanging drop method. AraCTP crystals grew in 50 mM Hepes, pH 5.5, 15% 2-propanol, 200 mM sodium citrate, and 10 mM magnesium chloride. dFdCTP crystals grew in 50 mM Hepes, pH 8.0, 20% 2-propanol, 200 mM sodium citrate, and 10 mM magnesium

chloride. dFdCTP crystals were further soaked in mother liquor containing 200 mM $MnCl_2$. Crystals were then transferred in four steps to a solution containing 25% ethylene glycol and flash-cooled. Data collection for both structures was performed at −178 °C on a Saturn92 CCD area detector mounted on a MicroMax-007HF (Rigaku Corp.) rotating anode generator equipped with Varimax HF mirrors. All data were processed using HKL2000. The structures were solved using molecular replacement using Protein Data Bank (PDB) entry 1XSN as a search model and using MOLREP (22). Refinement was carried out using CNS (23) and phenix (24), and model building was carried out with O (25) and Coot (26). The quality of the model was assessed using Molprobity (27), and it was found to have good stereochemistry (see Table 2).

Competition between dFdCTP and dCTP for Pol λ Incorporation—The same DNA oligonucleotides and reaction conditions as described above were used for competition study except for the concentrations of dCTP and dFdCTP. Under each dCTP concentration (0.1, 0.2, 0.5, 1, and 2 μM), increasing concentrations of dFdCTP (0, 0.5, 1, 5, and 20 μM) were added to the reactions. All of the kinetic data were determined based on the initial rate of the reactions under different combinations of dFdCTP and dCTP. The reaction mixtures were analyzed with a 12% denaturing polyacrylamide DNA sequencing gel, and the results were quantified with a phosphor imager (Fuji FLA5100).

RESULTS AND DISCUSSION

Incorporation of AraCTP and dFdCTP by Human Pol λ—The 39-kDa form of Pol λ was used in this study to allow direct comparisons of incorporation with crystal structures. To examine if AraCTP and dFdCTP are substrates, Pol λ was incubated with a DNA oligonucleotide substrate containing a one-nucleotide gap in the presence of

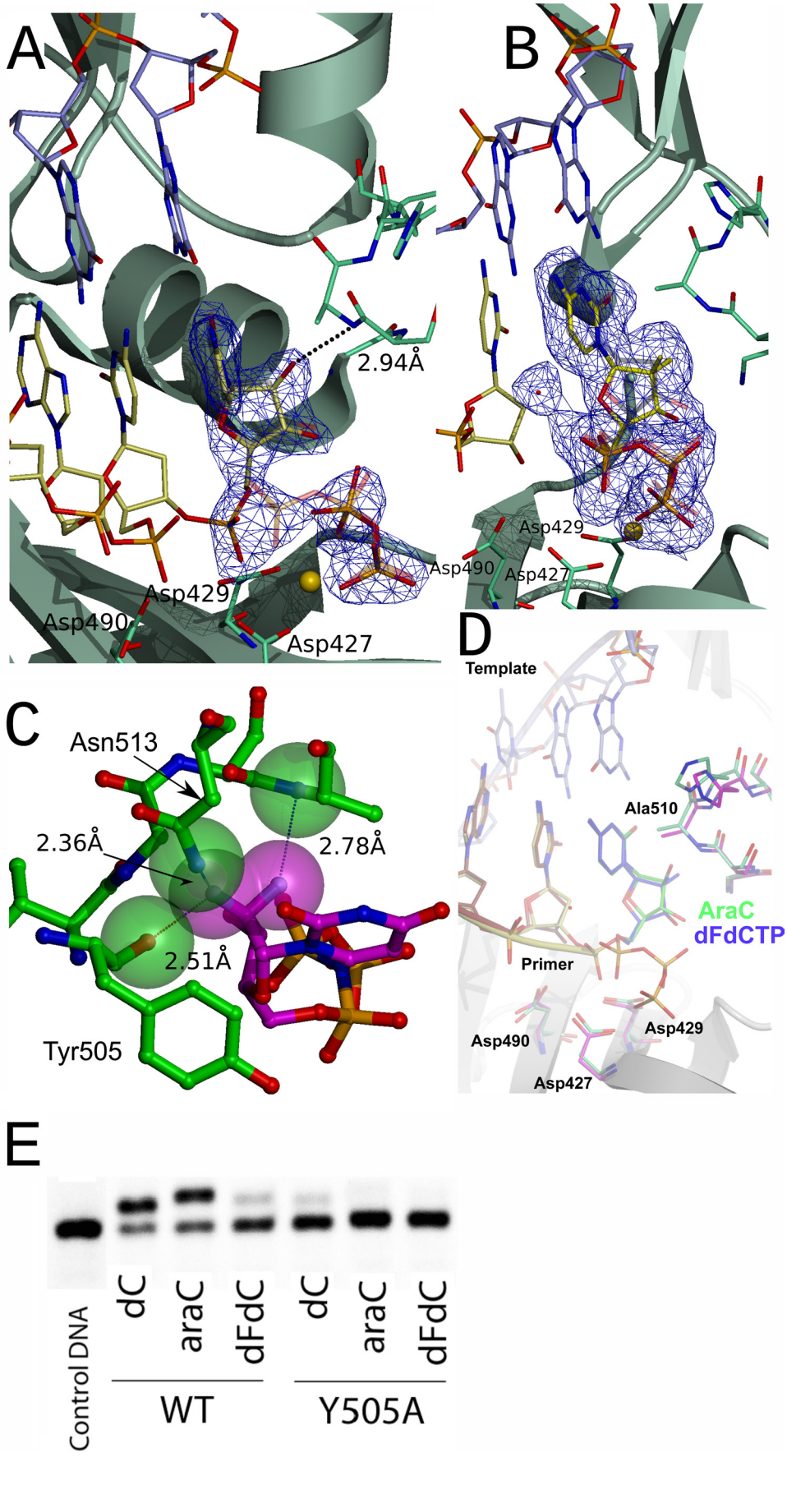

dCTP, AraCTP, or dFdCTP. As shown in Fig. 2, Pol λ inserted AraCTP into DNA, albeit slightly less efficiently than it incorporated dCTP. In contrast, dFdCTP was poorly inserted by Pol λ. Steady state kinetic analysis was then performed (Table 1). The K_m value of Pol λ for dCTP was 0.04 μM, and the k_{cat} was 7.0 min^{-1}. The incorporation efficiency (k_{cat}/K_m) for Pol λ on dCTP is 175. Compared with dCTP, Pol λ exhibited a higher K_m and a reduced k_{cat} (Table 1) when incorporating AraCTP, resulting in an 18-fold decrease in catalytic efficiency relative to dCTP. Incorporation of dFdCTP was even less efficient and was ~145-fold reduced as compared with dCTP.

Crystallization of Pol λ with Gapped DNA and Incoming Nucleoside Analogs—Several structures of Pol λ in complex with different DNA substrates and incoming nucleotides have resulted in a very detailed characterization of the polymerization reaction catalyzed by this enzyme (13, 28–33). Because AraCTP and dFdCTP are relatively similar substrates and yet Pol λ has a very different ability to incorporate them as shown in Fig. 2, we decided to co-crystallize Pol λ with either AraCTP or dFdCTP as incoming nucleotides to investigate the structural reasons for this difference. We therefore solved the co-crystal structures of Pol λ bound to a double-stranded DNA containing a single nucleotide gap and either AraCTP (2.03 Å) or dFdCTP (2.00 Å; see "Materials and Methods" and Table 2) as an incoming nucleotide. As shown in Fig. 3, *a–d*, both analogs can be accommodated in the dNTP binding pocket of the enzyme without major structural rearrangements. AraCMP was incorporated by the polymerase and is therefore observed as part of the growing chain. In contrast, very little incorporation of dFdCMP was observed, even after soaking the crystal in the presence of Mn^{2+} ions (see "Materials and Methods"). Both analogs appear to adopt a similar conformation. The main differences between these analog complexes and the reference structure with dCTP (PDB entry 2PFP) (28) are in the sugar moiety of the analogs. The 2′-OH of AraCTP is within hydrogen bonding distance of the backbone amide nitrogen of Ala^{510}. The presence of this atom does not appear to impose significant constraints in either the conformation of the ribose of the incoming nucleotide or the surrounding active site residues. On the other hand, the two fluorine atoms in C2′ of dFdCMP appear to be incompatible with the normal conformation of the ribose of the incoming nucleotide during catalysis. The dFdCMP ribose is shifted away from its usual position by about 0.9 Å, and it is apparent that if not for this shift, the fluorine atoms would clash with residues of the active site, in particular with the backbone carbonyl oxygen of Tyr^{505} and the delta nitrogen of Asn^{513}, which are 2.53 and 2.36 Å away, respectively, from one of the fluorine atoms in the structure. As a result of this shift, the α-phosphate of dFdCMP is slightly away from its normal catalytic position. Because the nucleophilic attack by the 3′-oxygen on the α-phosphate that is responsible for phosphoryl transfer is very sensitive to the geometry of the reactive groups, this difference can explain the observed reduction in catalytic efficiency with dFdCTP. Interestingly, discrimination against dFdCTP appears to be mostly based on the same structural features that allow Pol λ to discriminate against ribonucleotides. Previous studies suggested that amino acid Tyr^{505} plays an important role in polymerization and substrate selection (34–36). The impact of Tyr^{505} on the incorporation efficiency of AraCTP and dFdCTP was also examined using a Y505A mutant Pol λ. As shown in Fig. 3*e* and Table 3, the Y505A mutant has significantly reduced polymerase activity as compared with the wild type enzyme because its efficiency in incorporating dCTP is reduced more than 200-fold. Similar nucleotide selection preference was observed for the Y505A mutant as that of the wild type enzyme, which is dC > AraC > dFdC. As shown in the crystal structure, the side chain of Tyr^{505} does not appear to play a significant role in discriminating against dFdCTP, which is supported by the biochemical results. However, the Tyr^{505} side chain appears to play a general role in substrate selection. Although the structural basis for this role is not clear at present, it is possible that during the dNTP-induced conformational change, the side chain adopts a conformation not observed in the crystal structures that is critical for sugar discrimination. It is also possible that substitution of the tyrosine side chain might lead to local structural perturbations that affect sugar discrimination.

TABLE 3
The kinetic parameters of Y505A mutant Pol λ on dCTP and AraCTP

Substrate	k_{cat}	K_m	k_{cat}/K_m
	min^{-1}	μM	
dCTP	0.64 ± 0.06	0.81 ± 0.3	0.8
AraCTP	0.23 ± 0.01	2.3 ± 0.6	0.1
dFdCTP	0.26 ± 0.02	7.0 ± 1.6	0.04

Competition Assay between dFdCTP and dCTP—To obtain further information on the low efficiency of incorporation of dFdCMP, a competition assay was performed between dCTP and dFdCTP. Increasing concentrations of dFdCTP were added to the reactions containing a constant amount of dCTP. Fitting the results (Fig. 4) to a Michaelis-Menten equation revealed a mixed non-competitive mechanism of inhibition, where both the K_m and k_{cat} values changed with increasing concentration of dFdCTP (Table 4). The observed increase of K_m and reduction of k_{cat} in response to increasing concentrations of dFdCTP suggest that dFdCTP affects both the substrate binding and enzyme turnover. This is consistent with our structural obser-

FIGURE 3. **Structure of Pol λ in complex with AraCTP and dFdCTP.** *A*, the complex in which AraCTP is bound as an incoming nucleotide shows minimal distortion in the active site, and AraCMP has been fully incorporated into the primer chain. The AraCMP residue is overlaid with a normal dCTP residue (31). A simulated annealing $F_o - F_c$ electron density map contoured at 3σ is shown (*blue*). *B*, structure of Pol λ in complex with dFdCTP. Although dFdCTP can be bound in the Pol λ active site, it can only be accommodated in a conformation that differs significantly from that of a natural dCTP (*transparent*). A simulated annealing $F_o - F_c$ electron density map contoured at 3σ is shown (*blue*). *C*, two fluorine atoms have been modeled on the C2′ of a natural dCTP (31). The two fluorine atoms (Van der Waals surface in *magenta*) would clash with the backbone of active site residues and the side chain of Asn^{513} (*green*). *D*, an overlay view of AraCTP and dFdCTP within the active center of Pol λ. The primer strand of the AraC structure is *yellow*. The primer strand for the dFdCTP structure is *brown*. The three catalytic aspartates are shown in *magenta* (AraC) and *green* (dFdCTP). *E*, incorporation of AraCTP and dFdCTP by Y505A Pol λ mutant protein. The wild type or Y505A mutant Pol λ was incubated with a double-stranded DNA oligonucleotide in the presence of different nucleoside triphosphates at 37 °C for 3 min under the conditions described under "Materials and Methods."

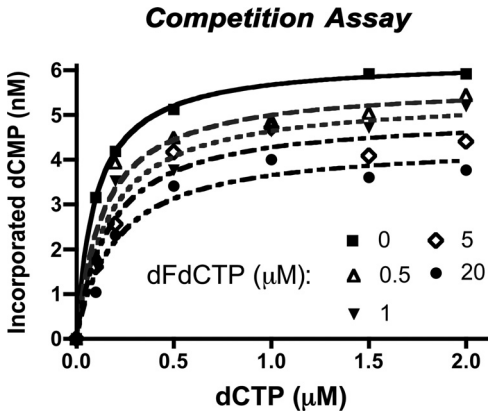

FIGURE 4. **The inhibitory effects of dFdCTP on the incorporation of dCTP by Pol λ.** The reaction conditions were the same as described under "Materials and Methods" except that increasing concentrations of dFdCTP (0, 0.5, 1, 5, and 20 μM) were added to the reactions of each dCTP concentration (0.1, 0.2, 0.5, 1, 1.5, and 2 μM).

TABLE 4

The kinetic parameters of pol λ on dCTP in the presence of increasing concentration of dFdCTP

	0 μM dFdCTP	0.5 μM dFdCTP	1 μM dFdCTP	5 μM dFdCTP	20 μM dFdCTP
k_{cat} (min^{-1})	6.2 ± 0.1	5.7 ± 0.3	5.4 ± 0.3	5.0 ± 0.2	4.4 ± 0.3
K_m (μM)	0.10 ± 0.01	0.14 ± 0.03	0.16 ± 0.04	0.17 ± 0.05	0.20 ± 0.06

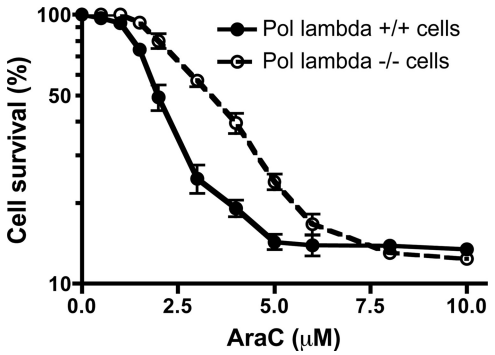

FIGURE 5. **Cell sensitivity of mouse Pol $\lambda^{+/+}$ and Pol $\lambda^{-/-}$ MEF cells to AraC.** The SV40-transformed Pol $\lambda^{+/+}$ and Pol $\lambda^{-/-}$ MEF cells were treated with increasing concentrations of AraC under the conditions described under "Materials and Methods." The cell survival data are presented as percentage of the absorbance of treated/untreated cells. *Error bars*, S.D.

vations, suggesting that the difluoro groups on the sugar moiety of dFdCTP affect the position of the α-phosphate.

Pol λ Affects Cellular Sensitivity to AraC—To further test whether Pol λ affects the cell sensitivity to AraC, MEF cells derived from either the wild type or Pol λ knock-out mice (19) were used to compare their sensitivity to AraC. As shown in Fig. 5, the Pol λ-deficient cells showed reduced sensitivity to AraC as compared with the wild type cells. This result is consistent with the biochemical and structural analysis and suggests that Pol λ plays a role in sensitizing cells to AraC *in vivo*.

In this study, we have reported the first co-crystal structure of a human DNA polymerase in complex with a nucleotide analog used for cancer therapy. These structures provide novel insight into the structural characteristics of these analogs that determine their efficient incorporation into DNA as well as the structural basis of sugar selectivity in Pol λ. Given the roles of Pol λ in DNA base excision repair and non-homologous end joining repair (21, 37), it is possible that the cellular sensitivity to AraC may partly depend on Pol λ. In particular, Pol λ may have a more profound impact on cellular sensitivity to AraC when used in combination with other DNA-damaging agents, such as mitoxantrone, which introduces DNA double strand breaks, and/or hydroxyurea or fludarabine, which affect cellular nucleotide pools.

REFERENCES

1. Balzarini, J. (1994) *Pharm. World Sci.* **16,** 113–126
2. Hiddemann, W. (1991) *Ann. Hematol.* **62,** 119–128
3. Burkes, R. L., and Shepherd, F. A. (1995) *Ann. Oncol.* **6,** Suppl. 3, S57–S60
4. Possinger, K. (1995) *Anticancer Drugs* **6,** Suppl. 6, 55–59
5. King, R. S. (1996) *Cancer Pract.* **4,** 353–354
6. Tanaka, M., and Yoshida, S. (1980) *Nippon Ketsueki Gakkai Zasshi* **43,** 996–1003
7. Huang, P., Chubb, S., Hertel, L. W., Grindey, G. B., and Plunkett, W. (1991) *Cancer Res.* **51,** 6110–6117
8. Plunkett, W., Huang, P., Xu, Y. Z., Heinemann, V., Grunewald, R., and Gandhi, V. (1995) *Semin. Oncol.* **22,** 3–10
9. Sommadossi, J. P. (1993) *Clin. Infect. Dis.* **16,** Suppl 1, S7–S15
10. Kufe, D. W., and Major, P. P. (1982) *Med. Pediatr Oncol.* **10,** Suppl. 1, 49–67
11. Mikita, T., and Beardsley, G. P. (1988) *Biochemistry* **27,** 4698–4705
12. Konerding, D., James, T. L., Trump, E., Soto, A. M., Marky, L. A., and Gmeiner, W. H. (2002) *Biochemistry* **41,** 839–846
13. Garcia-Diaz, M., Bebenek, K., Gao, G., Pedersen, L. C., London, R. E., and Kunkel, T. A. (2005) *DNA Repair* **4,** 1358–1367
14. García-Díaz, M., Bebenek, K., Sabariegos, R., Domínguez, O., Rodríguez, J., Kirchhoff, T., García-Palomero, E., Picher, A. J., Juárez, R., Ruiz, J. F., Kunkel, T. A., and Blanco, L. (2002) *J. Biol. Chem.* **277,** 13184–13191
15. Moon, A. F., Garcia-Diaz, M., Batra, V. K., Beard, W. A., Bebenek, K., Kunkel, T. A., Wilson, S. H., and Pedersen, L. C. (2007) *DNA Repair* **6,** 1709–1725
16. Garcia-Diaz, M., Bebenek, K., Larrea, A. A., Havener, J. M., Perera, L., Krahn, J. M., Pedersen, L. C., Ramsden, D. A., and Kunkel, T. A. (2009) *Nat. Struct. Mol. Biol.* **16,** 967–972
17. Joyce, C. M., and Steitz, T. A. (1994) *Annu. Rev. Biochem.* **63,** 777–822
18. Braithwaite, E. K., Kedar, P. S., Lan, L., Polosina, Y. Y., Asagoshi, K., Poltoratsky, V. P., Horton, J. K., Miller, H., Teebor, G. W., Yasui, A., and Wilson, S. H. (2005) *J. Biol. Chem.* **280,** 31641–31647
19. Braithwaite, E. K., Prasad, R., Shock, D. D., Hou, E. W., Beard, W. A., and Wilson, S. H. (2005) *J. Biol. Chem.* **280,** 18469–18475
20. Ohba, T., Kometani, T., Shoji, F., Yano, T., Yoshino, I., Ichiro, Y., Taguchi, K., Kuraoka, I., Oda, S., and Maehara, Y. (2009) *Mutat. Res.* **677,** 66–71
21. Capp, J. P., Boudsocq, F., Bertrand, P., Laroche-Clary, A., Pourquier, P., Lopez, B. S., Cazaux, C., Hoffmann, J. S., and Canitrot, Y. (2006) *Nucleic Acids Res.* **34,** 2998–3007
22. Vagin, A., and Teplyakov, A. (1997) *J. Appl. Crystallogr.* **30,** 1022–1025
23. Brünger, A. T., Adams, P. D., Clore, G. M., DeLano, W. L., Gros, P., Grosse-Kunstleve, R. W., Jiang, J. S., Kuszewski, J., Nilges, M., Pannu, N. S., Read, R. J., Rice, L. M., Simonson, T., and Warren, G. L. (1998) *Acta Crystallogr. D Biol. Crystallogr.* **54,** 905–921
24. Adams, P. D., Grosse-Kunstleve, R. W., Hung, L. W., Ioerger, T. R., McCoy, A. J., Moriarty, N. W., Read, R. J., Sacchettini, J. C., Sauter, N. K., and Terwilliger, T. C. (2002) *Acta Crystallogr. D Biol. Crystallogr.* **58,** 1948–1954
25. Jones, T. A., Zou, J. Y., Cowan, S. W., and Kjeldgaard, M. (1991) *Acta Crystallogr. A* **47,** 110–119
26. Emsley, P., and Cowtan, K. (2004) *Acta Crystallogr. D Biol. Crystallogr.* **60,** 2126–2132
27. Davis, I. W., Leaver-Fay, A., Chen, V. B., Block, J. N., Kapral, G. J., Wang, X., Murray, L. W., Arendall, W. B., 3rd, Snoeyink, J., Richardson, J. S., and Richardson, D. C. (2007) *Nucleic Acids Res.* **35,** W375–W383
28. Garcia-Diaz, M., Bebenek, K., Krahn, J. M., Blanco, L., Kunkel, T. A., and Pedersen, L. C. (2004) *Mol. Cell* **13,** 561–572
29. Lee, J. W., Blanco, L., Zhou, T., Garcia-Diaz, M., Bebenek, K., Kunkel,

T. A., Wang, Z., and Povirk, L. F. (2004) *J. Biol. Chem.* **279,** 805–811
30. Picher, A. J., García-Díaz, M., Bebenek, K., Pedersen, L. C., Kunkel, T. A., and Blanco, L. (2006) *Nucleic Acids Res.* **34,** 3259–3266
31. Garcia-Diaz, M., Bebenek, K., Krahn, J. M., Pedersen, L. C., and Kunkel, T. A. (2007) *DNA Repair* **6,** 1333–1340
32. Bebenek, K., Garcia-Diaz, M., Foley, M. C., Pedersen, L. C., Schlick, T., and Kunkel, T. A. (2008) *EMBO Rep.* **9,** 459–464
33. Cisneros, G. A., Perera, L., García-Díaz, M., Bebenek, K., Kunkel, T. A., and Pedersen, L. G. (2008) *DNA Repair* **7,** 1824–1834
34. Shevelev, I., Blanca, G., Villani, G., Ramadan, K., Spadari, S., Hübscher, U., and Maga, G. (2003) *Nucleic Acids Res.* **31,** 6916–6925
35. Crespan, E., Zanoli, S., Khandazhinskaya, A., Shevelev, I., Jasko, M., Alexandrova, L., Kukhanova, M., Blanca, G., Villani, G., Hübscher, U., Spadari, S., and Maga, G. (2005) *Nucleic Acids Res.* **33,** 4117–4127
36. Brown, J. A., Fiala, K. A., Fowler, J. D., Sherrer, S. M., Newmister, S. A., Duym, W. W., and Suo, Z. (2010) *J. Mol. Biol.* **395,** 282–290
37. Vermeulen, C., Bertocci, B., Begg, A. C., and Vens, C. (2007) *Radiat. Res.* **168,** 683–688